Clustering and defect structure of CaF_2 crystals doped with YbF_3 and ErF_3 as determined by ^{19}F nuclear magnetic resonance

R. J. Booth, M. R. Mustafa,* and B. R. McGarvey†
Department of Chemistry, University of Windsor, Windsor, Ontario, Canada N9B 3P4
(Received 13 January 1978)

^{19}F NMR studies of single crystals of CaF_2 doped with 2, 1, and 0.5 mole percent of both ErF_3 and YbF_3 have been carried out at room temperature. In ErF_3-doped crystals, ^{19}F resonances have been identified for lattice fluorides having both one and two Er^{3+} ions in nearest-neighbor cation sites and for an interstitial fluoride with two Er^{3+} ions in nearest-neighbor sites. In YbF_3-doped crystals, resonances have also been identified for lattice fluorides having both one and two Yb^{3+} ions in nearest-neighbor cation sites plus a fluoride with two nearby Yb^{3+} ions not in normal cation sites. Analysis of the results indicate that all the rare-earth ions are associated in some type of cluster at all concentrations studied and that the structure of these clusters does not agree with any model proposed in the literature. Comparison of these results with an earlier study of doped CdF_2 crystals shows that the same dopant produces a greater distortion of the cubic fluoride ion lattice in CaF_2 than in CdF_2.

I. INTRODUCTION

The work reported upon deals with doped CaF_2 crystals grown from a mixture of CaF_2 and rare-earth trifluorides under a fluorinating atmosphere. Many studies[1] of CaF_2 doped with rare-earth ions have been reported with the nature of the defect structure being determined or inferred mainly from optical, ESR, or electron-nuclear double resonance (ENDOR) studies. The many defects observed involving oxide ions and alkali-metal ions should not occur to any extent in the crystals used in this work. Instead we will be concerned with defect structures involving the interstitial fluoride ion and clustered rare-earth ions. CaF_2 has the fluorite structure which can be visualized as a cubic lattice of fluoride ions in which every other body-centered position is occupied by a divalent calcium ion. When rare-earth trifluorides are used as dopants, the trivalent rare-earth ions replace Ca^{2+} ions with the extra fluoride ion required for charge compensation occupying one of the vacant body-centered positions. At low doping concentrations (0.05 mol % or less) the rare-earth ion is found in sites of cubic, tetragonal, and (to a lesser extent) trigonal symmetry. The cubic sites are thought to be sites in which the charge-compensating interstitial fluoride ion lies far removed from the rare-earth ion while the tetragonal sites are assumed to have the interstitial ion in the adjacent body-centered position. ENDOR studies[2-4] on tetragonal sites for CeF_3, NdF_3, and YbF_3-doped crystals have confirmed the presence of the interstitial fluoride.

Since the ESR work of Bleaney *et al.*[5] and the x-ray work of Zintl and Udgard[6] and of D'Eye and Martin,[7] it has been commonly accepted that it is energetically favorable for charge compensation to occur locally, producing ion-defect pairs. The concentration of the ion-defect pairs depends upon the method of preparation of the crystal and Ure[8] has shown that the interstitial fluoride ion is not tightly bound to the rare-earth ion and can diffuse throughout the crystal at high temperatures. Friedman and Low[9] have utilized this F_i^- mobility to convert the local environment of the rare-earth ion from tetragonal to cubic symmetry.

There is considerable uncertainty and dispute as to what type of defects are found at higher doping concentrations. Weber and Bierig[10] suggested that the appearance of many new ESR lines in their CaF_2 crystals doped with ErF_3 or YbF_3 might be due to the presence of energetically favored pairs or clusters of ions. Naberhius and Fong[11] have calculated and Fenn, Wright, and Fong[12] have proposed (from optical data) that ion-defect pairs associate to form dimers as pictured in Fig. 1 or higher-order clusters. Neutron-diffraction studies on CaF_2 crystals doped with large concentrations of YF_3 led Cheetham and coworkers[13,14] to propose a distorted form of the dimer in Fig. 1 called the 2:2:2 cluster in which the two interstitial fluorides are only 200 pm apart and the two lattice fluorides labeled *a* in Fig. 1 are displaced along [111] axes to become essentially two more interstitial ions. For higher doping concentrations they propose a more extended cluster, called the 3:4:2 cluster, having four rare-earth ions. Catlow[15] has attempted to calculate the formation energy of such clusters and was able to rationalize the neutron-diffraction results. To explain the short distance between two interstitial fluoride ions, he proposed a

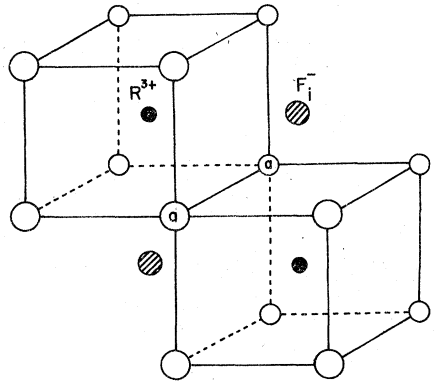

FIG. 1. CaF_2 lattice with two rare-earth ions (R^{3+}) substitutionally situated in the nearest-neighbor cation sites and the charge compensating fluoride ions (F_i^-) situated in the nearest-neighbor interstitial sites.

molecular orbital model in which the molecule ion F_2^{2-} is stabilized by delocalization of the two antibonding electrons into the conduction band of CaF_2. Evidence for clustering of the sort shown in Fig. 1 has been found by Kask and Kornienko[16] for Nd^{3+} in CaF_2 and SrF_2, who observed the ESR spectrum of an interacting pair of Nd^{3+} ions occupying nearest-neighbor sites along the [110] axis. Similar spectra were observed also by Baker and Marsh[17] for Tm^{2+} in CaF_2 and SrF_2 but in this case there is no need for the interstitial fluoride ions.

Tallant *et al.*[18] measured the concentration of tetragonal, trigonal, and several cluster sites for ErF_3 in CaF_2 using laser spectroscopy. They found that the concentration of tetragonal and trigonal sites decreased in concentration with increasing dopant concentration above 0.1% doping. Above 0.2% the concentration of cluster sites was an order of magnitude higher than that of tetragonal and trigonal sites. They could not measure the concentration of cubic sites and if one assumes an average of two Er^{3+} ions per cluster site the total concentration of all sites studied by Tallant *et al*,[18] would account for only 25% of Er^{3+} in the crystal.

Because the percentage of ions giving an ESR spectrum associated with cubic symmetry increases at higher dopant concentrations, Miner, Graham, and Johnston[19] and O'Hare[20] have postulated that, instead of dimers (as in Fig. 1) and related clusters being formed, a separate phase region is formed in which the cubic unit cell contains one rare-earth ion, three Ca^{2+} ions, one interstitial F^-, and the usual eight lattice fluorides. This new crystal structure has each rare-earth ion in a site of cubic symmetry but still has a nearby interstitial F^- providing local-charge compensation. This structure does not have rare-earth ions at adjacent sites and does not have the interstitial fluoride occupying a site adjacent to any rare earth ion.

Banks, Greenblatt, and McGarvey[21] and Mustafa *et al.*[22] have studied the ^{19}F NMR of CdF_2 crystals containing 10 mol% of ErF_3 and 6 mol% of YbF_3. They observed the resonance signals from lattice fluorides adjacent to the rare-earth ions plus an additional signal when the magnetic field was along the [100] axis that was attributed to an interstitial fluoride having two rare-earth ions in adjacent sites such that the R-F-R angle was 90°. This would be the situation for the defect dimer shown in Fig. 1. Intensity measurements showed that nearly all interstitial fluorides were accounted for in this signal. No resonances from the lattice fluorides adjacent to both rare earths in the dimer (ions a in Fig. 1) were observed.

Analysis[23] of ENDOR and NMR data[3,24] on the tetragonal site of Yb^{3+} in CaF_2 has shown considerable distortion of lattice fluorides from the cubic structure for the nearest fluoride ions. Catlow[15] predicted similar large distortions for the dimer pictured in Fig. 1. No distortions from a cubic structure were detected in the ^{19}F NMR of Er^{3+} and Yb^{3+} in CdF_2,[21,22] but the large linewidths in these crystals, caused by the large concentration of paramagnetic ions, would prevent detection of all but very large distortions.

In earlier studies of doped CdF_2 crystals[21,22] the contribution of an individual rare-earth ion to the paramagnetic shift of a nearby fluoride was analyzed using the equation

$$\Delta B/B_0 = -[a_s + (a_p + a_M)(3\cos^2\theta - 1)], \tag{1}$$

in which θ is the angle between the magnetic field and the vector connecting the rare-earth ion with the fluoride ion. ΔB is the difference between the resonant field of the nucleus and the resonant field of the reference nuclei (bulk lattice fluorides), a_s is the isotropic contribution from spin transfer, a_p is the anisotropic contribution from spin transfer, and a_M is the direct dipolar contribution of the metal ion, which in Système International units is

$$a_M = (\chi/R^3)\times 10^{-7}. \tag{2}$$

χ is the magnetic susceptibility per ion and R is the distance between the rare-earth ion and the ^{19}F nucleus. In the CdF_2 studies[21,22] it was found if one assumed χ to be given by the high-temperature limit

$$\chi = [g_J^2 J(J+1)\mu_B^2/3kT], \tag{3}$$

where g_J is the Landé g factor for the given rare-earth ion, μ_B the Bohr magneton, and the other symbols have their usual meaning, that a_p could

be taken to be negligible.

Theoretical calculations[25] of the ^{19}F NMR shift in CaF_2 and CdF_2 doped with YbF_3 using covalent mixing parameters determined by ENDOR and crystal-field levels determined by optical studies revealed that the correct value of χ at room temperature should be 79% of that predicted by Eq. (3). However, the covalent term a_p made a contribution of ~20% to give a shift very close to that predicted by Eqs. (2) and (3). Further, the calculations showed that the calculated value of a_M+a_p in CaF_2 would remain nearly invariant for any reasonable value of the crystal field. Less exact calculations for Er^{3+} in CaF_2 gave a similar result.

NMR studies on pure crystals of ErF_3,[26] HoF_3,[27] and TbF_3,[27] have shown that the anisotropic behavior of the NMR shift can be calculated within 10% using the known crystal structure plus Eqs. (1)–(3). In these crystals the average value of χ determined experimentally agrees very well with that given by Eq. (3). Equations (2) and (3) assume an isotropic susceptibility for the rare-earth ion. This would be true for a cubic site but not if the true symmetry were distorted. Susceptibility studies on TbF_3,[28] and on ErF_3,[29] reveal considerable anisotropy in the magnetic susceptibility even at 300 °K for these crystals. However, it has been shown[27] that agreement between theory and experiment is little changed from that obtained by assuming an isotropic susceptibility. In fact, it has been demonstrated[27] for both ErF_3 and TbF_3 that the difference (less than 10%) between the experimental anisotropic behavior of the NMR shift and the calculated behavior is mainly due to errors in the crystal structure used to make the calculations. Thus, all the experimental and theoretical results obtained so far indicate that the anisotropic behavior of the NMR shifts can be calculated by using a point-dipole model in which $a_p=0$ and a_M is given by Eqs. (2) and (3). This means we can extract useful structural data from the observed anisotropic behavior of ^{19}F NMR shifts of doped CaF_2 systems.

It was clear from the CdF_2 studies,[21,22] which showed the linewidths of the shifted lines to be field dependent, that improved resolution would be obtained in crystals having a lower doping concentration. Therefore, after improving the sensitivity of our spectrometer, we undertook a study of CaF_2 crystals doped with 0.5, 1.0, and 2.0 mol% ErF_3 and YbF_3.

II. EXPERIMENTAL

The NMR spectra were obtained using a broad-line spectrometer described elsewhere.[22,26] The frequency of the spectrometer was 46.6 MHz and all spectra were taken at room temperature (25 °C). For some of the very weak resonances detected, it was necessary to use integration time constants of 10–30 sec in the phase detector and sweep times of up to 4 h in order to obtain acceptable signal-to-noise. Shorter times were used for the bulk of the observed spectra.

The samples studied were cylindrical crystals of CaF_2 doped with either ErF_3 or YbF_3 in the nominal percentages of 0.5, 1.0, and 2.0 mol% and were supplied by Optovac, Inc., North Brookfield, Mass. The crystals were 10 mm in diameter and 20 mm in length with the cylindrical axis being either the [100] axis (0.5-mol% ErF_3, 2.0- and 0.5-mol% YbF_3) or the [110] axis (2.0- and 1.0-mol% ErF_3 and 1.0-mol% YbF_3).

The crystal holder was a 50-mm perspex rod of 12-mm diam with a 10-mm diam-hole drilled axially in the base. The crystal to be studied was glued inside the rod and a detection coil was tightly wound around and glued to this rod to obtain a good filling factor. The sample holder was rigidly mounted with the cylindrical axis vertical to the plane in which the magnetic field was rotated.

For all spectra the spectrometer frequency was determined with a frequency counter and the field sweep system was calibrated by a proton NMR spectrometer. Relative intensity measurements were made by numerical integration of the derivative curves obtained. When different portions of the spectrum required different gain settings, the gain settings were calibrated by comparing intensities of the bulk resonance signal (using a small enough modulation to allow display of spectrum on chart) at both gain settings.

III. RESULTS

A. ErF_3 in CaF_2

Spectra were recorded at 5° intervals through a 180° arc for rotations of the magnetic field in (100) and (110) crystal planes. The strong central line, due to fluoride ions far from the rare-earth ions, was used as an internal reference for measuring the shift ΔB. This shift is plotted as a function of angle for both rotation planes in Fig. 2. The data for the (110) plane come from both 1.0% and 2.0% crystals, since no discernible difference in resolution or spectra (except for the intensity of the shifted lines) could be found. The data for the (100) plane were obtained from the 0.5% crystal. The spectra along the [110] and [100] axes in the 0.5% crystal were identical to those found in the 1.0% and 2.0% crystals except for the change in intensity of the shifted lines rel-

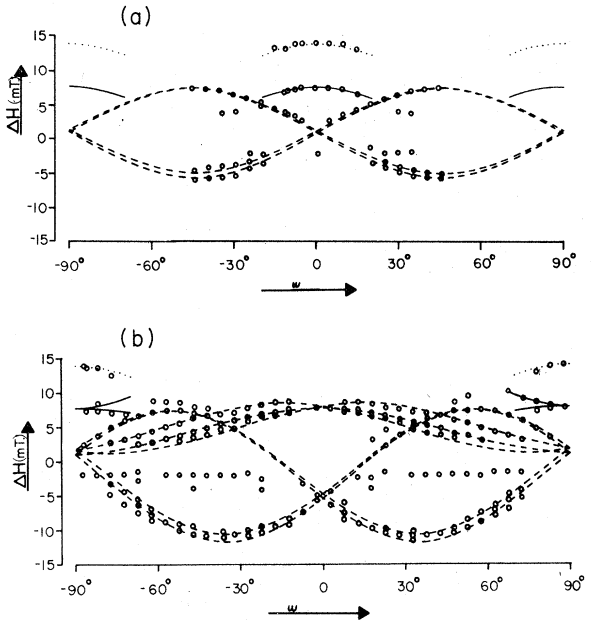

FIG. 2. Orientation dependence of various ^{19}F NMR lines at 46.6 MHz in CaF_2:ErF_3 crystals. (a) Angular dependence in the (100) plane as B_0 is rotated between [100] axes ($\omega = 0$ and $\pm 90°$). (b) Angular dependence in the (110) plane as B_0 is rotated from the [110] ($\omega = 0$) to the [100] ($\omega = \pm 90°$) axes.

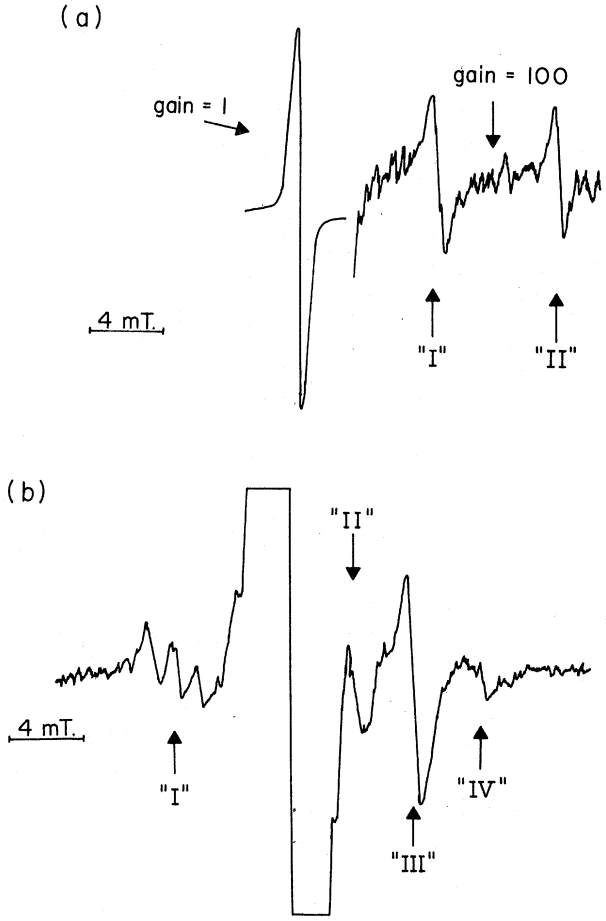

FIG. 3. Representative ^{19}F NMR spectra of CaF_2:ErF_3 crystals recorded at 46.6 MHz. (a) Spectrum when B_0 is parallel to the [100] axis. Line I is attributed to lattice fluorides with two nearest-neighbor erbium ions and line II is attributed to interstitial fluorides with two nearest-neighbor erbiums. (b) Spectrum when B_0 is 22° from the [100] axis in the (110) plane. Lines I, II, and III arise from lattice fluorides with only one nearest-neighbor erbium ion and line IV is attributed to a lattice fluoride with two nearest-neighbor erbium ions.

ative to the main center line.

Representative spectra are shown in Fig. 3 for the magnetic field parallel to [100] and at 22° to [100] in the (110) plane. When a weak line overlapped with a much larger line, as in Fig. 3, we took the line center to be the field at which the first derivative of the absorption curve crossed the zero base line. If it did not cross the base line then the field at which it came closest to the base line was used as the line center. Except for the case of severe overlapping, we have found this to be a useful and reasonably accurate way of estimating line centers for the weak satellite lines near to the large main resonance.

The points connected by dashed lines in Fig. 2 are the most intense satellites and by reason of their intensity and orientational behavior must be attributed to the lattice fluorides adjacent to one erbium ion. In the case of the three lines maximizing near or on the [110] axis, the dashed lines represent a least-squares fit of the function

$$\Delta B/B_0 = A\cos^2(\omega - \omega_{\max}) + B. \quad (4)$$

For the lines minimizing near each [111] axis, there are at least three separate lines. The two dashed lines represent the possible range of curves that might be fitted to the observed points. The best values for these fitted curves are given in Table I. Using the downfield lines observed when the magnetic field is along the [111] axis, we have computed their intensity relative to the total intensity of the ^{19}F spectrum and have found the percentage of fluorides adjacent to one erbium to be $6.0\% \pm 1.0\%$ for a 2-mol % crystal. This means that the number of fluoride ions (adjacent to only one erbium) per erbium ion is 6.1 ± 1.0 for 2 mol % crystals. For cubic sites in CaF_2 the ratio should be eight and for dimer sites the ratio is six fluorides per erbium ion.

In CdF_2:ErF_3 crystals, only three lines were observed[22] in the (110) plane for lattice fluorides

TABLE I. Least-squares fitted values[a] for rotation plots of resonances belonging to lattice fluorides having one rare-earth ion in a nearest-neighbor site.

Crystal	Rotation plane	10^3A	10^3B	ω_{max}
CaF_2:ErF_3	(100)	11.24	−4.84	±45.0°
		10.63	−4.22	±45.0°
	(110)	16.68	−10.29	±34.9°
		15.61	−9.22	±34.5°
		5.49	0.90	90.0°
		6.04	0.97	±76.3°
CaF_2:YbF_3	(100)	2.63	−1.08	±45.0°
	(110)	3.29	−2.02	±35.3°
		1.46	0.00	±90.0°
		1.77	0.08	±72.0°

[a]Plots fitted to Eq. (4). ω is angle to [100] axis. Errors in A and B are $\pm 0.04 \times 10^{-3}$.

adjacent to one erbium ion and only two lines in the (100) plane. Otherwise the results are very similar for the two lattices. If we take the average of the split lines in CaF_2 and compute values of a_s and $(a_p + a_M)$ from Eq. (1) we get

$$a_s = -(1.05 \pm 0.07) \times 10^{-3},$$

$$a_p + a_M = (5.41 \pm 0.04) \times 10^{-3},$$

which compare with the values

$$a_s = -(0.9 \pm 0.1) \times 10^{-3},$$

$$a_p + a_M = (4.85 \pm 0.09) \times 10^{-3},$$

found[22] for CdF_2:ErF_3. Presumably the higher concentration of ErF_3 in CdF_2 produced broader lines which prevented detection of the splitting observed here in CaF_2.

The lines appearing at ~ -2 mT in the (110) plot are strong lines that are barely detectable due to their closeness to the main resonance line. For reasons developed in Sec. IV, they have been assigned to lattice fluorides that are next-nearest neighbors to an erbium ion.

Two weaker resonances are seen near the [100] direction. The one connected by the dotted line has a shift and orientation behavior identical to that of a line observed in CdF_2:ErF_3 and attributed to an interstitial fluoride with two nearest-neighbor erbium ions located as in Fig. 1. Due to lower intensities in the CaF_2 crystals, the orientation behavior of this line could not be followed over as large an angular variation as was done for CdF_2. The intensity of this resonance in 2% crystals showed this fluoride ion to be $1.2\% \pm 0.6\%$ of all fluorides, that is, 1.2 ± 0.6 of these fluorides for every erbium ion. The second resonance near [100] connected by a solid line was not seen in the CdF_2 crystals. For reasons developed later in the paper we attribute this line to a lattice fluoride with two of the nearest-neighbor metal ion sites occupied by erbium ions. These fluorides are $1.5\% \pm 1.0\%$ of all fluorides in a 2% crystal which gives 1.5 ± 1.0 fluorides for every erbium ion. For the dimer pictured in Fig. 1, the ratio should be 1.0 for such a fluoride.

There are points in the upfield region of both plots that are not connected by any lines. In all cases these are very weak resonances that can barely be detected and for which no attempt was made to guess at any assignment.

B. YbF_3 in CaF_2

Plots of ΔB versus angle are given in Fig. 4 for the (110) plane and in Fig. 5 for the (100) plane. The data for (110) plane came from the 1.0% crystal while the data for the (100) plane is a combination of results for 0.5% and 2.0% crystals. As was the case in CaF_2:ErF_3 no difference was observed in the spectra for the three concentrations, except for the intensity of the satellite lines. Representative spectra are given in Fig. 6 for the magnetic field in the [100] and [110] directions.

The dashed lines connect points that by intensity and orientation behavior must belong to lattice fluorides adjacent to one ytterbium ion. The dashed lines are least-squares fitted according to Eq. (4) with the best values given in Table I. The behavior of these lines is qualitatively similar to that observed in CaF_2:ErF_3. The lines minimizing around [111] in the (110) plot are not split into several lines as was the case for ErF_3 doped crystals but the much smaller shifts observed in YbF_3 doped crystals make it less likely that such a splitting could be resolved. The three lines maximizing around [110] are found in both systems but the splitting is relatively larger for the

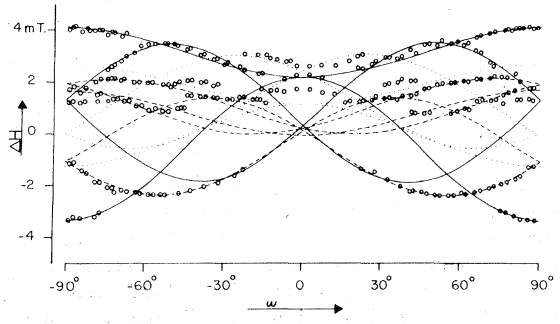

FIG. 4. Orientation dependence of various ^{19}F NMR lines at 46.6 MHz for the CaF_2:YbF_3 crystal in the (110) plane. B_0 is parallel to the [110] axis at $\omega = 0$ and parallel to the [110] axes at $\omega = \pm 90°$.

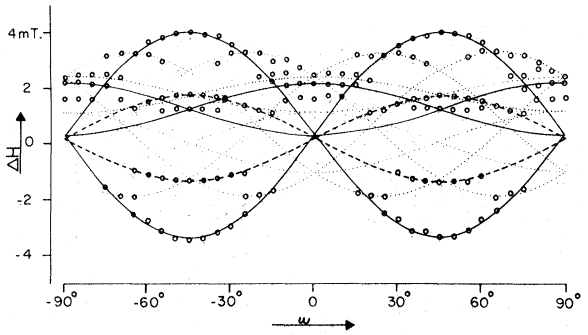

FIG. 5. Orientation dependence of various ^{19}F NMR lines at 46.6 MHz for the CaF_2: YbF_3 crystal in the (100) plane. B_0 is parallel to the [100] axes at $\omega = 0$ and $\pm 90°$ and parallel to the [110] axes at $\omega = \pm 45°$.

YbF_3 doped crystals. As with the ErF_3-doped crystals, if we use the average of the split lines in CaF_2 to compute values of a_s and $a_p + a_M$ from Eq. (1) we get

$$a_s = -(0.32 \pm 0.08) \times 10^{-3},$$

$$a_p + a_M = (1.17 \pm 0.04) \times 10^{-3},$$

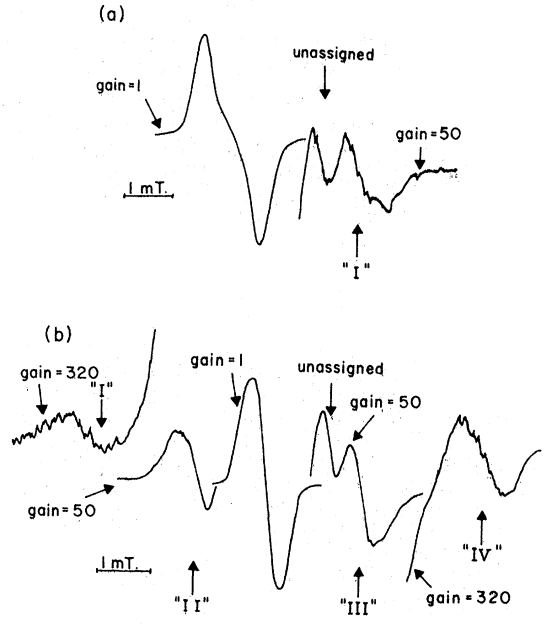

FIG. 6. Representative ^{19}F NMR spectra of CaF_2: YbF_3 crystals recorded at 46.6 MHz. (a) When B_0 is parallel to the [100] axis. Line I is a conglomerate of weak lines and one stronger line which arises from lattice fluorides with two nearest-neighbor ytterbium ions. (b) When B_0 is parallel to the [110] axis. Lines I and IV arise from the lattice fluorides with two nearest-neighbor ytterbiums and lines II and III arise from lattice fluorides with only one nearest-neighbor ytterbium ion.

which compare with the values

$$a_s = -(0.12 \pm 0.07) \times 10^{-3},$$

$$a_p + a_M = (1.06 \pm 0.04) \times 10^{-3},$$

found[22] for CdF_2:YbF_3. The intensity of these lines show the percentage of fluoride ions adjacent to one ytterbium to be $6.0\% \pm 1.0\%$ for the 2.0% crystals and $3.2\% \pm 1.0\%$ for the 1.0% crystals or a ratio of 6.1 ± 1.0 or 6.4 ± 2.0, respectively, for the number of fluoride ions per ytterbium ion.

The points connected by a solid line were not seen in the CaF_2:ErF_3 crystal or the CdF_2:YbF_3 crystal studied earlier.[22] They represent a species with a very anisotropic shift tensor in which one principal axis is along [100] and the two others are along mutually orthogonal [110] axes. The principal shift values are

$$(\Delta B/B_0)_{100} = (1.94 \pm 0.04) \times 10^{-3},$$

$$(\Delta B/B_0)_{110} = (3.54 \pm 0.04) \times 10^{-3},$$

$$(\Delta B/B_0)_{110} = -(2.87 \pm 0.04) \times 10^{-3}$$

The intensity of these lines give a value of $1.2\% \pm 0.6\%$ for the percentage of fluoride ions belonging to this species for the 2.0% crystal and $0.6\% \pm 0.3\%$ for the 1.0% crystals or a ratio of 1.2 ± 0.6 fluoride ions per ytterbium ion for both concentrations. As will be shown later in Sec. IV, the only possible explanation for these lines is a lattice fluoride with two adjacent sites occupied by ytterbium ions.

The dotted lines in both plots connect lines much weaker than those connected by the solid lines. The dotted lines were calculated assuming a species with principal shift values of

$$(\Delta B/B_0)_x = (2.90 \pm 0.04) \times 10^{-3},$$

$$(\Delta B/B_0)_y = -(1.59 \pm 0.04) \times 10^{-3},$$

$$(\Delta B/B_0)_z = +1.03 \times 10^{-3},$$

where the z axis is along a [100] axis of the crystal and the xz principal plane is 29.1° from a (100) plane. The x and y principal values are well determined by the (100) plot but the z value cannot be determined with any accuracy. It is clear it is somewhere between $+1.1 \times 10^{-3}$ and -1.1×10^{-3} with a slightly better fit for the positive values. The intensity of the lines could not be accurately measured due to their weakness and lack of good resolution from other lines. They certainly represent fluoride ions of considerably lower percentage than any discussed so far.

There are points in Figs. 4 and 5 that cannot be assigned to any of the three systems discussed up to now. The points at ~+1.5 mT near [110] and at ~+2.0 mT about 40° from [100] in the (110)

plot are intense enough to be due to lattice fluorides near one ytterbium ion. There are also points near [100] maximizing at

$$\Delta B/B_0 = (1.45 \pm 0.04) \times 10^{-3},$$

which cannot be lattice fluorides but could be some sort of interstitial fluoride.

IV. DISCUSSION

A. Fluoride ions with two nearest neighbors

The resonances represented by the solid line in Figs. 4 and 5 for CaF_2:YbF_3 vary so greatly with orientation that they must be due to fluoride ions close to at least two ytterbium ions. They are readily accounted for by assuming the fluoride ion is a regular lattice fluoride (such as ion a in Fig. 1) with two nearest-neighbor cation sites occupied by ytterbium ions. We assume a model of one fluoride ion with two equidistant rare-earth ions. The plane of the three ions is a (110) plane with the line joining the two rare-earth ions a [110] axis. If we let β be the angle between the metal-ion–fluoride-ion vector and the [100] axis in the plane of the three ions, we obtain the following equations for the principal shifts using Eqs. (1) and (2):

$$(\Delta B/B_0)_{100} = -a_s - 2a_M(3\cos^2\beta - 1), \quad (5)$$

$$(\Delta B/B_0)_{110} = -a_s + 2a_M, \quad (6)$$

$$(\Delta B/B_0)_{110} = -a_s - 2a_M(3\sin^2\beta - 1). \quad (7)$$

Equation (6) refers to the [110] axis perpendicular to the plane of the three ions and Eq. (7) refers to the [110] axis connecting the two rare-earth ions. a_M is given by Eq. (2) and a_s is again the isotropic component of the shift. The experimental principal shifts substituted into Eqs. (5)–(7) give

$$a_s = -0.87 \times 10^{-3}, \quad a_M = 1.34 \times 10^{-3}, \quad \beta = 63.5^\circ.$$

The a_M value is similar to the value found for a lattice fluoride adjacent to one ytterbium. Using Eqs. (2) and (3), a_M for a lattice fluoride adjacent to one ytterbium gives $R = 231$ pm which is close to the $Ca^{2+} - F^-$ distance of 236 pm. a_M for the lines attributed to a lattice fluoride adjacent to two ytterbium ions gives $R = 221$ pm. The a_s value is almost three times larger in magnitude than that for a fluoride ion adjacent to only one ytterbium ion. We would expect a_s for two ions to be double that for one ion when R is the same but for a smaller R value an even larger magnitude is quite reasonable.

Thus, the values of a_M and a_s are quite reasonable for our proposed model. The value of β, however, is not expected. For the cubic arrangement of a defect dimer as pictured in Fig. 1, β would be 54.7° if all ions occupied the sites in an undistorted fluorite lattice. In the dimer shown in Fig. 1, there are two lattice fluorides a adjacent to both rare-earth ions. Any symmetrical distortion of the system would keep both fluorides equidistant from both rare-earth ions. Using the value of β and the value of R obtained from a_M we find the distance between the two fluorides would have to be 197 pm which is much too short for two fluoride ions. We have tried to evaluate the effect of an anisotropic susceptibility on our results and conclude that an anisotropy consistent with the observed behavior of the resonances from fluoride ions adjacent to only one of the two ytterbium ions would not appreciably change any of the values of a_s, a_M, or β.

Catlow[15] has proposed a molecular-orbital model to explain the possible existence of two interstitial fluorides at a distance of 200 pm but it seems very unlikely that the presence of two rare-earth ions would cause two lattice fluorides to covalently bond to form an F_2^{2-} ion. We are, therefore, compelled to conclude that either the second fluoride ion is not there or the distortion is not symmetric and puts the second fluoride ion far enough away from the two rare-earth ions to give resonances that cannot be resolved from the main body of resonances in the spectrum. The second possibility is unlikely because it would produce much larger distortions, than those observed, in the behavior of the resonances associated with fluorides adjacent to only one ytterbium ion.

Although it is not yet clear what is the exact nature of the clustering going on in these crystals, it is certainly clear from the intensity of the resonances belonging to fluorides adjacent to two rare-earth ions that most of the ytterbium ions are present in some type of clusters at the doping concentrations studied. If doping were purely random in nature, we would expect the ratio of F^- ions having two Yb^{3+} ions as nearest neighbors to Yb^{3+} ions present to be 0.23 for 2% crystals, 0.12 for 1% crystals, and 0.06 for 0.5% crystals. The observed ratios are much larger than the statistical values, indicating a strong tendency towards clustering for the conditions used to prepare these crystals. Further the presence of these resonances at these intensities shows that clustering of the type proposed by Miner, Graham, and Johnston[19] and O'Hare[20] does not occur to any extent because their structure does not have any fluoride ions with two adjacent rare-earth ions.

These resonances do not confirm the presence of the 2:2:2 cluster proposed by Cheetham *et al.*[14] In this cluster the only fluoride ion with two close rare-earth-ion neighbors is the interstitial fluoride

but this fluoride with its two nearest rare-earth ions lie in a (100) plane rather than the (110) plane and would give the maximum upfield shift when the magnetic field is along the [100] axis rather than along the [110] axis observed for the resonance found in our studies. The 3:4:2 cluster of Cheetham is not ruled out because it does have four lattice fluorides each adjacent to two rare-earth ions.

The question arises as to why these resonances were not seen in CdF_2 and in CaF_2:ErF_3. In the case of CdF_2 the higher concentration of doping resulted in significant broadening of all lines due to random presence of paramagnetic ions outside the immediate vicinity of the fluoride nucleus. Since the resonances in CaF_2:YbF_3 were weak and already broader than all the other satellite lines, any additional broadening would make these lines impossible to detect with our present apparatus. We postulate that the lines are also present in CaF_2:ErF_3 but are too broad in most orientations to detect. The lines are broader in CaF_2:YbF_3 than other satellite lines, presumably due to a very effective relaxation mechanism involving two nearest-neighbor magnetic ions. If this is the case, then the much larger magnetic moments for Er^{3+} would produce much broader lines. For the CaF_2:YbF_3 system these lines are narrower in the region of the [100] direction and we postulate that the resonances connected by a solid line in Fig. 2 are indeed from the lattice fluorides adjacent to two Er^{3+} ions. It occurs in a reasonable region along the [100] axis and splits into two lines away from the [100] axis in the (110) plane. It also remains as a single line moving to lower fields in the (100) plane. Unfortunately this line broadens too much to obtain any other principal values of the shift tensor to confirm this assignment.

The weak lines connected by a dotted line in Figs. 4 and 5 exhibit such large shifts upfield and downfield that they have to come from a fluoride close to more than one ytterbium ion. The most reasonable explanation for these lines is a model in which a fluoride ion is adjacent to two rare-earth ions as for the resonances discussed above except that the plane of the three ions contains one [100] axis and makes an angle of $\pm(24.1\pm2.0)^\circ$ with a (100) plane containing this [100] axis. The two metal ions lie in a line perpendicular to this [100] axis. Using the same analysis above we obtain the values of

$$a_s = -0.78\times10^{-3},\quad a_M = 1.06\times10^{-3},\quad \beta = 57.2^\circ,$$

assuming $(\Delta B/B_0)_z = 1.03\times10^{-3}$. These are reasonable values for such a model. The other extreme value of $(\Delta B/B_0)_z = -1.03\times10^{-3}$ gives less reasonable values of $a_s = -0.09\times10^{-3}$, $a_M = 1.41\times10^{-3}$, and $\beta = 46.9^\circ$.

Although it is clear that these weak lines are best explained by our model, it is not at all clear what sort of defect structure or cluster would lead to two rare-earth ions in a (100) plane at basically the nearest-neighbor cation distance from each other but with the line connecting them making an angle of $\pm24^\circ$ to another [100] axis. No proposed defect or cluster in the literature would give rise to such an arrangement. The existence of these lines definitely show that more than one type of defect or cluster are present in CaF_2:YbF_3 at the concentrations studied.

B. Fluoride ions with one nearest neighbor

The dashed lines in Figs. 2, 4, and 5 have been assigned to lattice fluorides close to one rare-earth ion for both CaF_2:ErF_3 and CaF_2:YbF_3 by reason of their intensity, orientational behavior, and magnitude of shifts. For a perfect cubic site in which all nearest-neighbor fluorides are along radial vectors parallel to [111] axes we would expect only three lines in a (110) plot and two in a (100) plot. Such is obviously not the case for the two systems studied here. Splittings, as observed here, could result from distortions which make the radial vectors no longer parallel to [111] axes of the crystal. If no other rare-earth ions were nearby, however, we would expect the maximum upfield shift for every line to be the same in our plots no matter what the nature of the distortion from cubic symmetry. This is observed not to be the case for both systems studied. Different maxima could result from an anisotropy in the ionic susceptibility χ or from the presence of a second rare-earth ion in the vicinity.

In Fig. 7 are given the calculated curves for fluoride ions with one nearest-neighbor and one next-nearest-neighbor Er^{3+} ion; here we have used Eqs. (1)–(3) with $a_s = 0$ and have assumed an undistorted lattice as pictured in Fig. 1. Although the curves are not identical to those measured, it becomes clear that the observed curves could probably be explained by some sort of distortion from cubic symmetry plus the presence of other rare-earth ions in the next-nearest-neighbor cation sites. The distortion of radial vectors from the [111] directions do not seem to be great however. We have not tried to determine the exact form of distortion necessary to predict the observed curves because we have no way of estimating the extent of anisotropy in the magnetic susceptibility of the rare-earth ion.

In the preceding calculation we can also calculate the orientational behavior of fluorides that

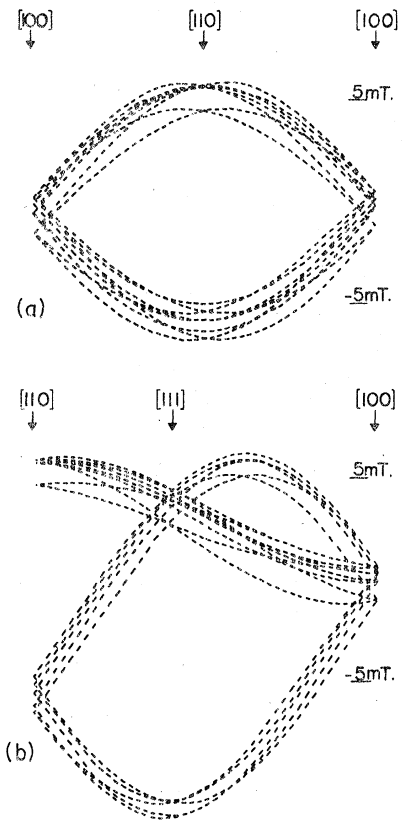

FIG. 7. Calculated orientational behavior of ^{19}F NMR lines, at 46.6 MHz, for lattice fluorides with one nearest-neighbor and one next-nearest-neighbor erbium ion. Here we have used Eq. (1)–(3) with $a_s = 0$ and have assumed an undistorted lattice as shown in Fig. 1. (a) is the predicted (100) plot and (b) is the predicted (110) plot.

only have rare-earth ions in next-nearest-neighbor cation sites. This calculation shows for the (110) plane a series of lines minimizing around −2.3 mT for Er^{3+} at 46.6 MHz. We therefore feel that the lines observed at ~ −2.0 mT for CaF_2:ErF_3 are due to such fluorides.

Although we cannot, as yet, pinpoint the nature of the distortion in CaF_2, we can make a comparison of the effect of a given ion in the CaF_2 lattice versus that in the CdF_2 lattice. If splittings of the lines, attributed to lattice fluorides adjacent to one rare earth, observed in CdF_2 were of the same magnitude in CaF_2 we would expect to have seen some indication of this in the CdF_2 spectra even though the lines were considerably broader. No indication of deviation from cubic symmetry was seen in CdF_2, however. Further, comparison of the average values of $a_M + a_p$ determined in both lattices reveals larger values in CaF_2 for both ErF_3 and YbF_3 doping. If we assume $a_p = 0$ and use Eqs. (2) and (3) to calculate the metal-ion–fluoride-ion distance, we get the results given in Table II. It should be noted that R is smaller for CaF_2 than for CdF_2 even though the normal cation-anion distance is larger in CaF_2 than CdF_2. Since the ionic radii[30] of Er^{3+} and Yb^{3+} are considerably smaller than either Ca^{2+} or Cd^{2+}, we can explain these results only by postulating that the cubic lattice of fluoride ions in CdF_2 is more resistant to deformation than in CaF_2. This is possibly explained by the fact that the distance between fluoride ions is smaller in CdF_2 than in CaF_2.

TABLE II. Calculated values of rare-earth-ion–fluoride-ion distances in doped CaF_2 and CdF_2.

	CaF_2	CdF_2
Yb^{3+}-F^- distance (pm) [a]	231 ± 3	238 ± 3
Er^{3+}-F^- distance (pm) [a]	228 ± 1	236 ± 1
M^{2+}-F^- distance (pm) [b]	237	233

[a] Calculated from Eqs. (2) and (3) assuming $a_p = 0$.
[b] Normal cation-anion distance in pure crystal.

C. Interstitial fluorides

The dotted line in Fig. 2 near the [100] axis was detected[22] in CdF_2:ErF_3 also and assigned to an interstitial fluoride with two nearest-neighbor cation sites occupied by Er^{3+} ions. To explain the orientational behavior it was necessary to assume the two vectors connecting the interstitial fluoride with the two Er^{3+} ions were at right angles as would be the case for the defect dimer pictured in Fig. 1. This still seems to us to be the best explanation for this line.

A weak broad upfield line was also detected[22] along [100] for CdF_2:YbF_3 and assigned as the same interstitial fluoride even though its orientational behavior could not be followed. This line was found in the region where the solid and dotted lines intersect along [100] in Figs. 4 and 5 for CaF_2:YbF_3. It is now clear that the line assigned to an interstitial fluoride in CdF_2:YbF_3 is in fact from a lattice fluoride adjacent to two ytterbium ions. Either the interstitial fluoride signal observed in CaF_2:ErF_3 is not there or it occurs in the vicinity of the dotted lines along [100] in Figs. 4 and 5 distorting the positions of these lines. We consider the latter situation the more probable. The unassigned resonance maximizing along [100] at $\Delta B/B_0 = (1.45 \pm 0.04) \times 10^{-3}$ behaves like an interstitial fluoride but its upfield shift is not large enough to assign it to a fluoride with two nearest-neighbor ytterbium ions unless a_s is taken to be negative. Its shift is about right for an interstitial fluoride with only one ytterbium ion in a nearest-neighbor cation site. This line is observed, how-

ever, over too small a region to make any definitive assignment.

V. CONCLUSIONS

This work shows that a careful NMR investigation of single crystals doped with rare-earth ions can be a powerful tool in studies of how the lattice is distorted in the vicinity of the impurity ion. In the case of CaF_2 this study has created as many questions as answers, so it is important to spell out here, what has been learned.

(i) For CaF_2 doped with ErF_3 or YbF_3, clustering in some form involves most of the rare-earth ions at concentrations of 0.5-mol % or better. This agrees with the results of Tallant *et al.*[18] on CaF_2:ErF_3 and Cheetham et al.[14] on CaF_2:YF_3.

(ii) For both ErF_3 and YbF_3 this clustering is definitely not of the type proposed by Miner, Graham, and Johnston[19] or O'Hare[20] and, also, not the 2:2:2 cluster proposed by Cheetham[14] and developed by Catlow.[15] The results are not inconsistent with the 3:4:2 cluster proposed by Cheetham for concentrations over 10 mol%, although the upfield shift for the interstitial fluoride for B_0 along the [100] axis should not be as large as that observed for Er^{3+} in both CaF_2 and CdF_2. Further it is clear from our studies that more than one type of cluster is probably present in the crystals studied.

(iii) Distortions of the cubic lattice of fluoride ions are larger in CaF_2 than in CdF_2 for the same dopant ions.

The main question left unanswered is the structure or nature of the cluster or clusters. We have been unable, as yet, to devise a model that satisfies both our results and the neutron diffraction studies of Cheetham *et al.*[14] The 3:4:2 cluster of Cheetham *et al.* comes close but they only proposed this cluster for concentrations an order of magnitude larger than the crystals we studied.

We are currently extending our studies to CaF_2 crystals doped with rare-earth ions of larger ionic radii than Er^{3+} or Yb^{3+} to see if the results obtained here are found for all rare-earth ions, or if the nature of defects and extent of clustering is critically dependent on the size of the rare-earth cation.

ACKNOWLEDGMENTS

This work was supported by a grant from the National Research Council of Canada.

---

*Present address: University of Khartoum, Khartoum, Sudan.

†Author to whom requests for reprints should be sent.

[1]See, *Crystals with the Fluorite Structure*, edited by W. Hayes (Clarendon, Oxford, 1974).

[2]J. M. Baker, E. R. Davies, and J. P. Hurrell, Proc. R. Soc. A 308, 403 (1968).

[3]J. M. Baker, E. R. Davies, and T. Rs. Reddy, Phys. Lett. 29 A, 118 (1969).

[4]D. Kiro and W. Low, *Magnetic Resonance*, edited by C. K. Coogan, M. S. Hain, S. N. Stuart, J. R. Pilbrow, and G. V. H. Wilson (Plenum, New York and London, 1970), pp. 247-269.

[5]B. Bleaney, P. M. Llewellyn, and D. A. Jones, Proc. Phys. Soc. B 69, 858 (1956).

[6]E. Zintl and A. Udgard, Z. Anorg. Chem. 240, 150 (1939).

[7]R. W. M. D'Eye and F. S. Martin, J. Chem. Soc. 349, 1847 (1957).

[8]R. W. Ure, J. Chem. Phys. 26, 1363 (1957).

[9]E. Friedman and W. Low, J. Chem. Phys. 33, 1275 (1960).

[10]M. J. Weber and R. W. Bierig, Phys. Rev. 134, A1492 (1964).

[11]S. L. Naberhius and F. K. Fong, J. Chem, Phys. 56, 1174 (1972).

[12]J. B. Fenn, Jr., J. C. Wright, and F. K. Fong, J. Chem. Phys. 59, 5591 (1973).

[13]A. K. Cheetham, B. E. F. Fender, D. Steele, R. J. M. Taylor, and B. T. M. Willis, Solid State Commun. 8, 171 (1970).

[14]A. K. Cheetham, B. E. F. Fender, and M. J. Cooper, J. Phys. C 4, 3107 (1971).

[15]C. R. A. Catlow, J. Phys. C 6, 64 (1973); *ibid.* 9, 1859 (1976).

[16]N. E. Kask and L. A. Kornienko, Fiz. Tver. Telz. 9, 2291 (1967) [Sov. Phys.-Solid State 9, 1795 (1968)].

[17]J. M. Baker and D. Marsh, Phys. Lett. A 35, 415 (1971).

[18]D. R. Tallant, D. S. Moore, and J. C. Wright, J. Chem. Phys. 67, 2897 (1977).

[19]G. K. Miner, T. P. Graham, and G. T. Johnston, J. Chem. Phys. 57, 1263 (1972).

[20]J. M. O'Hare, J. Chem. Phys. 57, 3838 (1972).

[21]E. Banks, M. Greenblatt, and B. R. McGarvey, J. Chem. Phys. 58, 4787 (1973).

[22]M. R. Mustafa, W. E. Jones, B. R. McGarvey, M. Greenblatt, and E. Banks, J. Chem. Phys. 62, 2700 (1975).

[23]B. R. McGarvey, J. Chem. Phys. 65, 955 (1976).

[24]J. P. Wolfe and R. S. Markiewizc, Phys. Rev. Lett. 30, 1105 (1973).

[25]B. R. McGarvey, J. Chem. Phys. 65, 962 (1976).

[26]M. R. Mustafa, B. R. McGarvey, and E. Banks, J. Magn. Reson. 25, 341 (1977).

[27]A. Reuveni and B. R. McGarvey, J. Magn. Reson. 29, (1978).

[28]L. Holmes and H. J. Guggenheim, J. Phys. (Paris), Colloq. C1-501 (1971).

[29]P. E. Hansen (private communication).

[30]*Handbook of Chemistry and Physics*, 49th ed., edited by R. C. Weast (The Chemical Rubber Co., Cleveland, Ohio, 1968), pp. F-152-53.